Observation of many-body effects in positron annihilation in alkali metals

S. M. Kim* and A. T. Stewart†
Department of Physics, University of North Carolina, Chapel Hill, North Carolina
(Received 12 August 1974)

The momentum distribution of photon pairs from positrons annihilating in lithium, sodium, potassium, and rubidium has been measured over a wide temperature range. The results were analyzed to yield the momentum dependence of the enhancement factor, positron effective mass, and positron minimum energy in these metals. The annihilation rate at the Fermi momentum was found to be considerably higher than that at zero momentum. The magnitude of this momentum dependence of enhancement factor as well as its variation with the electron density are in good quantitative agreement with the many-body theoretical calculations. Assuming free-particle behavior, the positron effective mass has been determined to be approximately $1.8m$ in lithium and sodium, $2.1m$ in potassium, and $2.3m$ in rubidium. Using a more realistic momentum distribution for the positron, which includes the positron-phonon interaction, the effective mass observed for sodium would be about 1.4–1.6 in fair agreement with a calculation yielding 1.2. The thermalization of positrons was observed to be complete before annihilation down to—for example in Na—$160m/m^*$ °K. Below this temperature positrons seem to annihilate with certain minimum effective temperatures or minimum energies. These results are compared with theoretical calculations of the thermalization time of positrons in metals.

I. INTRODUCTION

Positron annihilation has been studied for some time mainly to gain information about the electron momentum distribution in solids.[1,2] Accurate angular-correlation measurements on oriented single crystals of Be,[3,4] Li,[5,6] Cu,[7,8] Si,[9,10] rare-earth,[11,12] and transition metals[13,14] revealed marked anisotropies in the photon momentum distribution, and these observed anisotropies were explained in terms of the band structure and the Fermi surface in these metals. An increased attention has been given to this field recently after a direct observation of the Fermi surface of copper by Fujiwara and Sueoka,[7] and the observation of vacancies in metals by MacKenzie *et al.*[15] Positron-annihilation angular-correlation measurements have now been extended to various alloys[16–20] to determine the Fermi surface of concentrated alloys, which cannot be measured with the more standard techniques such as the de Haas–van Alphen effect.[21] The observation of vacancies and dislocations in solids resulted in the development of a new tool for measuring the vacancy formation energies in metals[22–24] and alloys,[25] vacancy-solute binding energies,[23,26] radiation damage,[27,28] and annealing studies[27,29] in various materials. The usefulness of positron-annihilation technique in studying the Fermi surface in metals lies in part in the general assumption that positrons are thermalized before annihilation and the positron-electron interaction do not disturb appreciably the momentum distribution of electrons being investigated. Although the earlier angular-correlation measurements in simple metals[30] supported the validity of these assumptions, detailed investigations were needed as the experimental technique improved and the measurements became more precise.

The positron behavior in metals is fundamentally a many-body problem involving a distinguishable test charge immersed in the Fermi sea of electrons, and thus is of considerable interest by itself.[31] A number of many-body theoretical calculations have been made during the past several years on the annihilation rate of the positron,[32–37] positron effective mass,[38–40] and thermalization time[41–43] in simple metals. These calculations will be described briefly in this section together with the experimental observations which have been reported.

A. Enhancement factor: Polarization of electron gas

The annihilation rate of positrons in metals, which is given by the inverse of positron lifetime, is directly proportional to the electron density at the positron position.[32] Earlier measurements of positron lifetimes in simple metals showed that the annihilation rates were higher by a factor of 5–20 than those calculated from the Sommerfeld free-electron model.[44] The first successful theoretical calculations on the annihilation rate were done by Kahana, who included the many-body interaction of the positron with the electron gas.[33] This calculation has been refined by several authors during recent years.[34–37] These many-body calculations showed a large enhancement of electron density at the positron position, and also yielded a momentum dependence of enhance-

ment. The momentum dependence of enhancement was attributed to the Pauli exclusion principle, which inhibits the positron interaction with electrons deep inside the Fermi sea.

The experimental observation of the momentum dependence of enhancement was made on sodium by Donaghy and Stewart, who found that the annihilation rate at the Fermi momentum was about 60% greater than that at zero momentum.[45] A much weaker momentum dependence of enhancement was observed in aluminum by Berko and Erskine,[10] in qualitative agreement with Kahana's calculations. However, a detailed study of the variation of the momentum dependence of enhancement with the electron density has not been made.

B. Positron effective mass

It is trivial to show that, although the thermal smearing of the sharp break at the Fermi momentum due to electron motion is too small to be observed, the thermal motion of the positrons causes an appreciable smearing which can be observed with present precision.[46] An experiment designed to observe the positron motion was carried out on sodium by Stewart and Shand.[46,47] Using a high-resolution angular-correlation apparatus, they have measured the photon pair momentum distribution in sodium at various temperatures (110, 300, 400, and 600 °K). The results were analyzed assuming a free-electron model and a Gaussian momentum distribution for positrons. They found that positrons are thermalized at these temperatures, but the effective mass of the positron in sodium was about twice the electron mass.

The positron effective mass in metals will be different from the electron mass due to positron interactions with the ionic lattice, phonons, and electrons. The band effective mass of the positron has been calculated by us,[47] and also by Majumdar,[48] in sodium and some other metals. It was shown that $m^*_{\text{band}}/m = 1.05$ in sodium, slightly increasing in heavier elements. The phonon part of the positron effective mass was calculated by Mikeska,[49] and also by Perkins and Carbotte,[50] who showed that m^*_{phonon}/m is unity within a few percent in sodium. The positron effective mass in an electron gas was calculated by Hamann,[38] and also by Bergersen and Pajanne,[39] who obtained $m^*_{\text{electron}}/m = 1.15$ and 1.10, respectively, in sodium. Combining these results we obtain $m^*/m = 1.2$ in sodium, which is much too small to explain the observed effective mass of 1.8 ± 0.2. Some authors have shown that further broadening of the positron momentum distribution is expected if positron–phonon interactions are taken into account.[40,49] These calculations will be discussed in Sec. V.

C. Positron thermalization

High-energy positrons (~0.7 MeV) entering a metal lose their energy quickly through interactions with the ions, electrons, and phonons. The time required for the positron to reach a few electron volts of energy can be estimated to be about 10^{-16} sec.[51] In this initial stage the positron loses energy mainly by ionization of the inner-shell electrons of the ions. The low-energy positron further thermalizes through interactions with electrons and phonons in metals. The thermalization time τ of the positron due to interactions with the electron gas was first calculated by Lee-Whiting, who obtained $\tau \approx 3\times10^{-12}$ sec in sodium at room temperature.[41] Carbotte and Arora have refined this calculation and obtained $\tau = 1.3\times10^{-11}$ sec in sodium at room temperature.[42] They have also shown that τ increases considerably at low temperatures and in denser metals. Since the positron lifetime in metals is of order $(2-3)\times10^{-10}$ sec, it was suggested that positron thermalization may not be complete before annihilation at low temperatures. Positron thermalization due to phonons has been studied by Mikeska, who showed that in sodium the positron-phonon interaction dominates the thermalization process at below about 230 °K.[49] More detailed calculations by Perkins and Carbotte also gave similar results,[50] indicating that positron thermalization will be nearly complete in most metals, even at low temperatures.

In this paper we report high-resolution angular-correlation measurements in alkali metals Li, Na, K, and Rb over a wide temperature range (15–650 °K). Experimental data were analyzed to yield the momentum dependence of the enhancement factor, positron effective mass, and the minimum effective temperature or minimum energy at low temperatures. In Sec. II the photon angular distribution expected at finite temperatures is described. The experimental procedure and the data analysis are presented in Secs. III and IV, respectively. The results are discussed in Sec. V. A preliminary account of this work has been published previously.[52]

II. PHOTON MOMENTUM DISTRIBUTION

The annihilation rate of a low-energy positron with emission of a photon pair of total momentum $\vec{p}$ is given by[33]

$$R(\vec{p}) = (\lambda/V)\int d^3x\, d^3y\, e^{-i\vec{p}\cdot(\vec{x}-\vec{y})} G_{ep}(\vec{x}t, \vec{x}t; \vec{y}t^+, \vec{y}t^+), \tag{1}$$

where $\lambda = 5.05 a_0^3 \times 10^{10}$ sec^{-1} (a_0 is the Bohr radius) and G_{ep} is the electron-positron–pair Green's function. If we neglect the electron-positron in-

teractions $R(\vec{p})$ reduces to [32]

$$R(\vec{p}) = \lambda \sum_{\vec{k}} \left| \int \psi_{\vec{k}}(\vec{x})\psi_{+}(\vec{x})e^{-i\vec{p}\cdot\vec{x}}\, d^3x \right|^2, \qquad (2)$$

where $\psi_{\vec{k}}(\vec{x})$ and $\psi_{+}(\vec{x})$ are the electron and positron wave functions, respectively, and the summation extends over all occupied electron states $\vec{k}$. In alkali metals the annihilation rate of ion-core electrons is very small compared with that of conduction electrons, due to the ionic repulsion of the positron and the small core sizes. This component together with some high-momentum photon pairs arising from the Bloch character of the electron and positron wave functions gives rise to a broad distribution in the observed angular-correlation curves.

Free-particle plane-wave approximation for the electron and positron wave functions give a momentum distribution of

$$R_{\text{free}}(\vec{p}) = (\lambda/V)\Theta(1-p), \qquad (3)$$

where $\Theta(1-p)$ is a step function equal to 1 for $p \leq 1$ and zero otherwise and p is measured in units of the Fermi momentum. The many-body calculations of $R(\vec{p})$ by Kahana and other workers[33-36] give

$$R(\vec{p}) = (\lambda/V)\Theta(1-p)\epsilon(p), \qquad (4)$$

where $\epsilon(p)$, the momentum-dependent enhancement factor, may be characterized by $\epsilon(p) = a + bp^2 + cp^4$. This result was obtained by assuming that positrons are thermalized and annihilate in an electron gas at zero temperature. At finite temperatures $R(\vec{p})$ will be smeared by the thermal motion of electrons and positrons. The smearing due to electron motion is of order $(T/T_F)p_F$, where T_F is the Fermi temperature, and can be neglected compared to that due to the positron motion. Since there is only one positron in a metal at a given time, the momentum distribution of thermalized positrons can be taken as a Boltzmann distribution,

$$g(\vec{p}, T) = (2\pi m^* k_B T)^{-2/3} e^{-p^2/2m^* k_B T}, \qquad (5)$$

where m^* is the positron effective mass and k_B is the Boltzmann constant. Since the annihilation photons carry the combined momentum of the electron-positron pair, the momentum distribution at finite temperatures will be given by the convolution of $R(\vec{p})$ and $g(\vec{p}, T)$:

$$\begin{aligned} &R(\vec{p}, T) \\ &= (\lambda/V)\int R(\vec{p}\,')g(\vec{p}-\vec{p}\,', T)d^3p' \\ &= \tfrac{1}{2}[1 + \operatorname{erf}((1-p)/\beta)]F(p)[\beta/2(\pi p)^{1/2}]e^{-(1-p^2)/\beta^2}G(p), \end{aligned} \qquad (6)$$

where

$$F(p) = (\lambda/V)[a + \tfrac{3}{2}b\beta^2 + \tfrac{15}{4}c\beta^4 + (b + 5c\beta^2)p^2 + cp^4];$$

$$\begin{aligned} G(p) = (\lambda/V)[&a + b + c + (b + 2c)\beta^2 + 2c\beta^4 \\ &+ (b + c + \tfrac{7}{2}c\beta^2)p + (b + c + \tfrac{9}{2}c\beta^2)p^2 + c(p^3 + p^4)]; \end{aligned}$$

$$\operatorname{erf}(x) = (2/\sqrt{\pi})\int_0^x e^{-x^2}dx, \quad \beta = (2m^* k_B T)^{1/2}/p_F .$$

The coincident-photon-pair counting rate measured with a long slit apparatus at $p = p_z$ is given by a double integral of $R(\vec{p}, T)$ over p_x and p_y components. If we take into account the optical resolution of the apparatus $S(p_z)$, the coincident-photon-pair counting rate $N(p_z, T)$ and its slope can be reduced to the following form after some algebraic manipulations:

$$N(p_z, T) = \int dp\, I(p_z - p, T)\int_p^\infty dp\, 2\pi p R(p), \qquad (7)$$

$$\frac{dN(p_z, T)}{dp_z} = -2\pi \int dp\, I(p_z - p, T)pR(p), \qquad (8)$$

where

$$I(p_z, T) = \int dp\, S(p_z - p)g(p, T). \qquad (9)$$

The function $I(p_z, T)$ describes the combined effect of the apparatus resolution and positron motion. When this function is approximated by a Gaussian, Eqs. (7) and (8) can be integrated, and expressions very similar to (6) can be obtained.[53]

III. EXPERIMENTAL PROCEDURE

The angular-correlation measurements were made on lithium, sodium, potassium, and rubidium at various temperatures ranging from 15 to 650 °K. The coincident photon pairs were counted with NaI(Tl) detectors placed behind narrow slits 250 in. away from the sample. All measurements were made with slit openings of 0.050×24 in. except rubidium at 16 °K, which was measured with a 0.030×24-in. opening. One of the detectors was moved in regular steps on an arc centered near the sample position. The full angular range of interest was swept through in a few hours and this "scanning" repeated several times. The data from each such scan were examined to detect malfunction of the equipment and then the number of coincident counts obtained was summed for each angle. A fast twofold (35 nsec) and slow threefold coincidence system was used for the detection of coincident photons.

Since the alkali metals are soft and chemically active, considerable care was taken in handling the specimen. Reagent-grade metal samples of lithium, sodium, and potassium were cut to a

disk form ($\frac{1}{2} \times \frac{3}{16}$ in.) and rinsed in alcohol. A smooth and finished surface was obtained by lapping the specimen on a soft cloth stretched on a flat surface and wetted with methanol (for Li) or isopropanol (for Na and K). The samples were frequently cooled in xylene bath during the lapping procedure. The specimen was further etched in alcohol solution in xylene before transferring to the sample chamber. The rubidium sample (99.8% purity) was obtained in a glass ampoule, which was opened under dry mineral-oil bath. The sample was melted and transferred to a thin-wall aluminum specimen holder ($\frac{1}{2}$-in.-diam disk) using a syringe. A smooth surface was obtained by pressing the sample on a plate glass and etching in xylene.

The specimen was placed between the pole pieces of an electromagnet (Magnion Model UF-5) so that the positrons emitted from a ^{64}Cu foil (1.5 Ci) could be focused to a small area of the sample surface. Focusing positrons improved the stray-positron shielding problem and allowed capture of most positrons emitted into the solid angle 2π. The surface of the specimen was visually aligned with the slits. A gas-refrigerator-type cryostat was used for low-temperature measurements.[53] This apparatus consisted of vacuum-jacketed transfer lines leading from the storage Dewar of liquid helium or liquid nitrogen to the interior of the specimen holder made of a copper block, and terminating at the exit needle valve. The specimen and the specimen holder were radiation shielded by surrounding with copper sheets which were thermally attached to the appropriate exit vapor line. The specimen temperature was measured with an Allen-Bradley carbon resistor and a thermocouple, and was maintained constant within a few degrees by adjusting the pumping rate of the liquid coolant at the exit needle valve. For measurements at room temperature and above, an apparatus similar to that described previously[47] was used. A nichrome heater element was attached underneath the specimen holder, which was made of a thin-wall stainless-steel cup. All the measurements were carried out in vacuum except liquid sodium at 600 °K, which was done in argon atmosphere to decrease evaporation.

IV. ANALYSIS OF EXPERIMENTAL DATA

The angular-correlation data obtained in a series of measurements on alkali metals at various temperatures are plotted in Fig. 1. These data have been corrected for the decay of the positron source and plotted on one side of the symmetry axis $\theta = 0$. The total coincident counts accumulated at the centroid position ranged from about

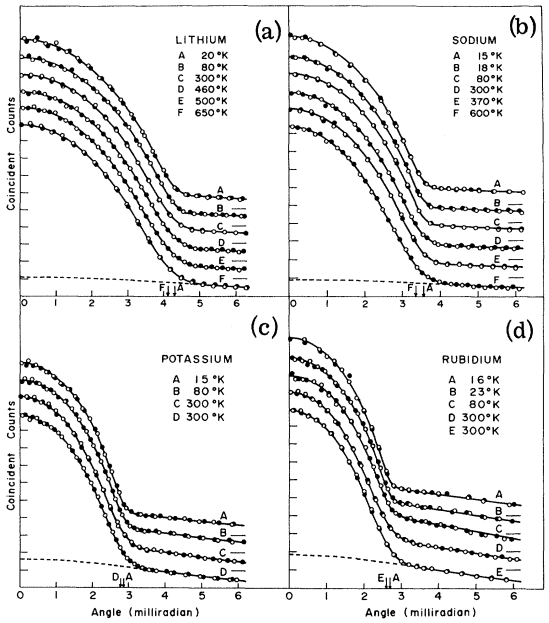

FIG. 1. Angular distribution of photons in lithium (a), sodium (b), potassium (c), and rubidium (d) at various temperatures indicated. The full lines are theoretical fits to the data assuming a Gaussian background as explained in the text.

13 000 to 30 000 counts. Thus the standard deviation of the counting statistics is about the size of the circles representing the data points. The photon angular distribution in these metals consists of a parabolic-shaped distribution arising from the conduction-electron annihilation superimposed upon a broad background. This background arises from the core-electron annihilations and the annihilation of the conduction electrons and the positron in higher-momentum states. The random coincident counts and the oxide film on the sample surface (notably in rubidium at 80 °K) also contributed small amounts to the background. The curvature at the end of the parabolic portion where it joins the broad background is caused mainly by the optical resolution of the apparatus and by the positron motion. As the temperature was increased, the smearing of the curve also increased. The Fermi cutoff ($\theta_F = p_F/mc$) decreases with temperature due to the lattice expansion, and is indicated with arrows in the abscissa. The solid curves drawn through the data points are visual fits to the data with theoretical curves calculated from Eq. (7) assuming a Gaussian distribution for the background.

A detailed shape of the angular distribution near the Fermi momentum can be seen more clearly in the slope presentation. Some of the derivatives of the coincident photon counting rate are plotted

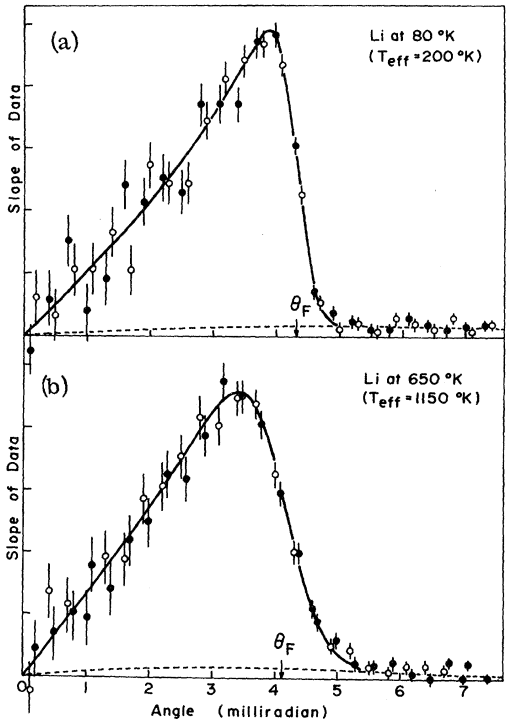

FIG. 2. Slope of the photon angular distribution in lithium at 80 °K (a) and 650 °K (b). The full lines are theoretical fits to the data as explained in the text.

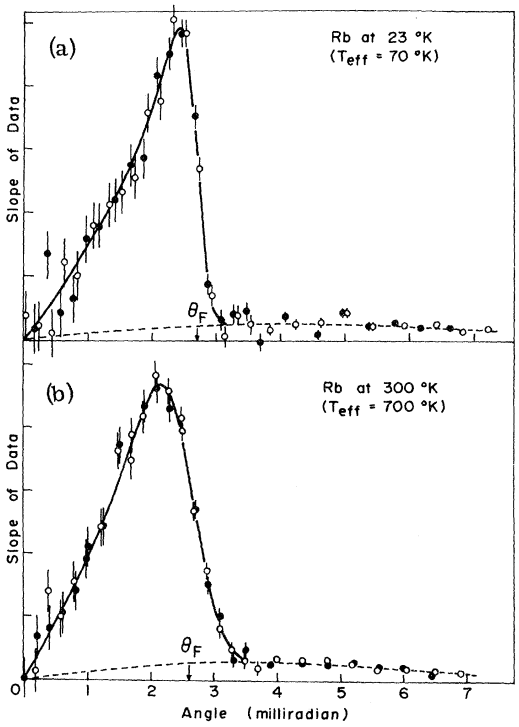

FIG. 3. Slope of the photon angular distribution in rubidium at 23 °K (a) and 300 °K (b). The full lines are theoretical fits to the data as explained in the text.

in Figs. 2 and 3. The solid curves drawn through the data points are visual fits to the data with curves calculated from Eq. (8), and the dashed lines indicate the assumed background. For convenience the background was assumed to be a Gaussian to be determined at large angles. Although the exact shape of the background at small angles is not known, as long as it varies smoothly the present results are not affected by any appreciable amount.

The optical resolution of the instrument arises from the finite slit openings at the photon detectors and positron penetration in the sample. The resolution effect of the slits can be described by a triangular function with a FWHM (full width at half-maximum) equal to the angle subtended by the slit. The positron intensity distribution at the sample was obtained assuming an exponential absorption[54] and allowing for the sample misalignment of order 0.01 in. across the $\frac{1}{4}$-in.-diam area where the positrons were focused. The optical resolution is given by the convolution of these two functions, and was calculated numerically on a computer for each sample at various measured temperatures. Since the penetration depth of 0.66-MeV positrons in alkali metals is of order 0.01–0.02 in., the optical resolution was dominated by the detector slits. The FWHM of the optical resolution ranged from 0.24 mrad in rubidium to 0.32 mrad in lithium with 0.05-in. slit openings. Thus the optical resolution caused a smearing of the data equivalent to the positron motion at 60 °K in rubidium and 100 °K in lithium. The positron momentum distribution at finite temperatures was assumed to be a Boltzmann distribution characterized by one parameter, $T_{\rm eff}$, which we call the positron effective temperature,

$$g(\vec{p}, T_{\rm eff}) = (2\pi m k_B T_{\rm eff})^{-3/2} e^{-p^2/2mk_B T_{\rm eff}} . \qquad (10)$$

For the thermalized positrons it is expected that $T_{\rm eff} = (m^*/m)T$, where m^* is the positron effective mass and T is the specimen temperature. The combined resolution effect of the instrument and positron motion, given in Eq. (9), was calculated on a computer and was approximated by a Gaussian, which it closely resembled. Equations (7) and (8) were then integrated to obtain expressions similar to that given in Eq. (6).[53] By varying the enhancement factors b/a and c/a as well as the positron effective temperature, a number of curves were calculated and compared with the data. Some of these curves obtained for potassium are plotted in Fig. 4.

Most of the observed angular-correlation data

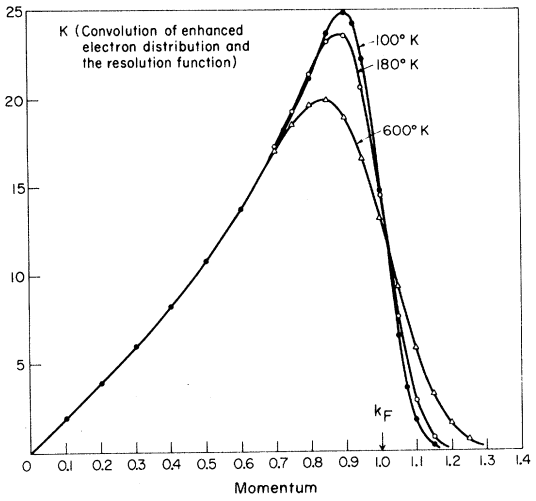

FIG. 4. Calculated slopes of the photon angular distribution for potassium, obtained from Eq. (8) with $b/a = 0.42$ and $c/a = 0.31$, at various positron effective temperatures.

could be fitted well with the calculated curves using the Fermi momentum obtained from the tabulated x-ray lattice-constant data[55] and densities in these metals. Since the Fermi momentum obtained from the density data is not expected to be accurate, the Fermi momentum was independently determined from the present data for all temperatures and compared with the expected values (Table I). The experimental accuracy of the cutoff angle is better than 1% for all solid specimens and is about $1\frac{1}{2}$% in liquid specimens. The overall close agreement between the observed and expected Fermi momentum confirms the calculations by Majumdar, who showed that the Fermi momentum is not shifted by electron-positron interactions.[56]

V. RESULTS AND DISCUSSION

A. Enhancement factor

The enhancement factors b/a and c/a, which characterize the momentum dependence, were mainly determined from the low-temperature data where the smearing due to the positron motion was negligible. Both the angular distribution and its slope were fitted consistently to obtain the best values of the enhancement factor. The values obtained are given in Table II. The experimental accuracy of $b/a + c/a$ was estimated to be 10% of the values given in the table, and this error arises mainly from the statistics of the data. Since the momentum dependence of enhancement varies as $1 + (b/a)p^2 + (c/a)p^4$, it was difficult to determine the values of b/a and c/a separately. Although the low-temperature data on sodium, potassium, and rubidium gave a slightly improved fit when b/a is reduced by 10% and c/a is increased by a corresponding amount, the high-temperature data gave a slightly better fit when the opposite change was made. These changes are, however, within the statistics of the data, and no appreciable temperature-dependent change of the enhancement factor was noted in all solid specimens. The angular distribution obtained in liquid lithium and sodium showed a much weaker momentum depen-

TABLE I. Fermi momentum p_F, in units of $(mc)^{-1}$ mrad determined from the data is compared with that obtained from the lattice-constant data and densities, p_F(calc).

Element	Temperature (°K)	p_F/mc (obs)	p_F/mc (calc from lattice and density)
	20	4.31 ± 04	4.31
Li	80	4.31 ± 04	4.31
	300	4.26 ± 04	4.29
	460	4.21 ± 04	4.22
	500	4.18 ± 06	4.2
	650	4.12 ± 06	4.2
Na	15	3.56 ± 04	3.56
	80	3.55 ± 04	3.55
	300	3.50 ± 04	3.51
	370	3.48 ± 04	3.47
	600	3.36 ± 05	3.4
K	15	2.88 ± 03	2.88
	80	2.87 ± 03	2.87
	300	2.80 ± 03	2.82
Rb	16	2.69 ± 03	2.69
	80	2.68 ± 03	2.68
	300	2.60 ± 03	2.63

TABLE II. Momentum dependence of the enhancement factor, $\epsilon(p) = a[1 + (b/a)p^2 + (c/a)p^4]$, determined from the data is compared with those obtained from the papers of Kahana (Ref. 33) and Carbotte (Ref. 35). The values in parentheses are smooth extrapolations to the corresponding electron densities.

Element	b/a	c/a	Kahana (Ref. 33) b/a	Kahana (Ref. 33) c/a	Carbotte (Ref. 35) b/a	Carbotte (Ref. 35) c/a
Li	0.27	0.19	0.22	0.17	0.22	0.23
Na	0.34	0.22	0.26	0.23	0.26	0.32
K	0.42	0.31	(0.32)	(0.32)	0.31	0.48
Rb	0.46	0.35	(0.34)	(0.36)	(0.33)	(0.54)

dence, i.e., $b/a = 0.2$ and $c/a = 0.1$, indicating some effect of the disorder on the momentum distribution. The enhancement factors obtained from the calculations of Kahana[33] and Carbotte,[35] by a smooth extrapolation to the electron density corresponding to these metals, are also given in Table II. Other calculations[34,36] give a very similar momentum dependence of annihilation rate with only slight variations in absolute magnitude. The present measurements give a good agreement with these calculations both in magnitude and in variation with the electron density. The much weaker enhancement factors observed in liquid Li and Na will be discussed in Sec. VI in connection with the possible positron localization at vacancies in liquid Li and Na before annihilation.[57]

B. Positron effective mass

The positron effective temperatures obtained by visual fits to the data with calculated curves are plotted against the specimen temperatures in Fig. 5. Since the positron motion mainly causes a smearing of the angular distribution near the Fermi momentum, the slope representation was more convenient in determining the positron effective temperatures. The statistics of the data and the imprecise knowledge of the background shape and the apparatus resolution caused some uncertainty in T_{eff}, and these were estimated and indicated in the figures. The positron effective temperature is seen to be linear with the specimen temperature, except at low temperatures, in all the metals studied. This linearity can be taken as a good evidence of positron thermalization at these temperatures. Assuming the positron is thermalized, the slope of the plots of T_{eff} versus T should be equal to the positron effective mass. The positron effective mass thus obtained is given in Table III. It is seen that the positron effective mass is about 1.8m in Li and Na and increases to 2.1 and 2.3m in K and Rb, respectively.

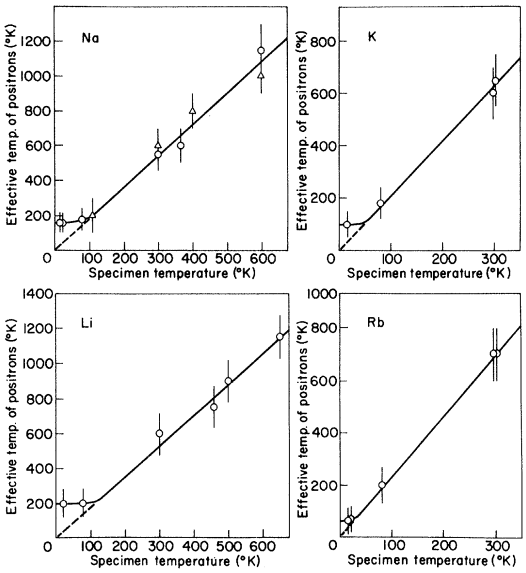

FIG. 5. Effective temperature of positrons vs the specimen temperature in lithium, sodium, potassium, and rubidium.

Since the positron interacts with the lattice, phonons, and electrons in solids, the observed positron effective mass will be given by

$$m^*/m \approx (m^*/m)_{\text{band}}(m^*/m)_{\text{phonon}}(m^*/m)_{\text{electron}}. \quad (11)$$

Theoretical calculations of the positron effective mass in sodium due to positron-lattice,[47,48] positron-phonon,[49,50] and positron-electron[38,39] interactions gave $m^*/m = 1.2$, as described in Sec. I. A slight increase in m^*/m is expected in K and Rb, since both the band effective mass, which depends on ionic size, and the electron-positron correlation effective mass, which depends on r_s, should increase in these metals. These calculated values are, however, too small to explain the large observed positron effective mass. One possible source of the discrepancy was discussed by Mikeska, who showed that the positron-phonon interactions causes an appreciable high-momentum tail in the positron momentum distribution, thus making the observed m^*/m larger than the calculations.[49] Bergersen and Pajanne have studied this problem in detail and concluded that this phonon effect would increase the observed positron effective mass by about (15–30%) in sodium.[40] The departure of the Fermi surface from a free-electron sphere in Li and Rb could also cause some additional smearing in the photon momentum distribution. We have estimated that these effects are, however, very small and within the error estimates given in Table III.

It is known that in many metals positron trapping at thermally generated vacancies causes

TABLE III. Positron effective mass and minimum energy (in T_{eff} °K and $k_B T_{\text{eff}}$ eV) determined from the present work.

Element	m^*/m	Minimum temperature (°K)	Minimum energy (eV)
Li	1.8±0.3	200±80	0.017±0.007
Na	1.8±0.2	160±50	0.013±0.004
K	2.1±0.3	100±60	0.008±0.005
Rb	2.3±0.3	60±50	0.005±0.004

narrowing and smearing of the angular distribution.[2] Theoretical calculations by Hodges indicate that positron trapping may occur in alkali metals.[58] He obtained the positron-vacancy binding energy in the alkali metals of about 0.1 eV, which is very small compared with those in other metals. His calculations, however, neglect the large relaxation of the atoms surrounding the vacancy and the reduction of the electron-positron correlation energy at vacancies. Inclusion of these two effects could easily wipe out the positron trapping in alkali metals, as discussed by Seeger.[24] Indeed, MacKenzie *et al.* have measured the positron lifetime in alkali metals as a function of temperature from 4 to 445 °K and found no evidence of positron trapping.[59] Present angular-correlation measurements also showed no change in the Fermi momentum except that due to the thermal expansion. Both measurements thus indicate that positron trapping does not occur in alkali metals in the solid state. In liquid Li and Na we observed an appreciable narrowing of the angular distribution, as manifested by a much weaker momentum dependence of the enhancement factor. Coupled with the observations by Brandt and Waung[57] of a 5% increase in positron lifetime across the melting point in sodium, it seems very likely that the positron is partially localized at vacancies in liquid alkali metals. As can be seen in Fig. 5, however, the positron effective mass determined solely from the solid-state measurements would not be different from the values given in Table III.

C. Positron thermalization

The plot of the positron effective temperature against the specimen temperature (Fig. 5) shows that T_{eff} is not linear with the specimen temperature at low temperatures. This nonlinearity can be taken as an evidence of incomplete positron thermalization at these temperatures of the ground-state motion of the positron in these metals. Positron thermalization seems to be complete at temperatures above about 100 °K in Li, 80 °K in Na, 50 °K in K, and 30 °K in Rb. Below these temperatures positrons seem not to thermalize completely and annihilate with certain minimum effective temperatures, or minimum energies. The observed minimum T_{eff} and the corresponding minimum energy obtained from the data assuming a Boltzmann distribution for the positron momentum are also shown in Table III.

As described in Sec. I, the high-energy positron (~0.7 MeV) entering a metal loses its energy quickly by ionization of the atoms, and reaches a few electron volts energy in about 10^{-16} sec.[51] Further thermalization occurs mainly due to collisions with the electron gas. The time required for the positron to reach a thermal energy E is given by the formula[42]

$$\tau(E) = \frac{105}{64me^4}\left(\frac{\hbar k_s^2}{2mE}\right)^2, \tag{12}$$

where k_s is the screening length. Using $k_s = 1.02\times10^8$ cm^{-1}, Lee-Whiting obtained $\tau(0.025\ \text{eV}) \simeq 3\times10^{-12}$ sec in sodium.[41] Carbotte and Arora have calculated the thermalization time in an electron gas using a random phase approximation, and showed that k_s should be fixed to the Thomas-Fermi value ($k_s^2 = 0.66 r_s k_F^2$).[42] They have obtained $\tau(0.025\ \text{eV}) = 1.3\times10^{-11}$ and $\tau(0.01\ \text{eV}) = 1.0\times10^{-10}$ sec in sodium. Compared with the observed positron lifetime in this metal of 3×10^{-10} sec,[44] it was suggested that positron thermalization may not be complete at low temperatures. Woll and Carbotte extended the above calculations and obtained the positron momentum distribution at low temperatures.[43] They found that at low temperatures positrons annihilate with certain minimum effective temperatures, as observed experimentally. They obtained a minimum T_{eff} of 64.3 °K in Li, 49.0 °K in Na, 39.2 °K in K, and 37.5 °K in Rb. Compared with the experimental values given in Table III, the agreement is poor although not inconsistent for K and Rb. Since at low temperatures positron-phonon interactions contribute significantly in shortening the thermalization time,[50] the disagreement of the observed and calculated minimum T_{eff} would be greater. One possible source of this discrepancy could be the phonon-induced high-momentum tail in the positron momentum distribution, which was shown to increase at low temperatures.[49] A detailed calculation by

Hede and Carbotte,[60] however, shows that the phonon contribution to the smearing is very small compared with the observed smearing at low temperatures. Another possible source of discrepancy is the martensite transformation in Li and Na, which occurs at about 78 and 35 °K, respectively.[61] This phase transformation, however, seems to have little effect on the photon momentum distribution, since the angular distribution remained unchanged below 80 °K in both Li and Na. Positron lifetime measurements also showed no changes down to 4 °K.[59] Thus the observed finite smearing at low temperatures in Li and Na remains unexplained. Further precise measurements and calculations are clearly needed for complete understanding of this result.

VI. CONCLUSIONS

The photon angular distribution has been measured in the alkali metals Li, Na, K, and Rb over a wide temperature range. The results were analyzed to yield information about the momentum dependence of the enhancement factor, positron effective mass, and minimum effective temperature.

The annihilation rate at the Fermi momentum was found to be greater than that at zero momentum by about 46% in Li, 56% in Na, 73% in K, and 81% in Rb. This is in good agreement, both in magnitude and variation with the electron density, with the many-body electron-gas calculations by Kahana and other workers.

The free-particle positron effective mass was found to be about $1.8m$ in Li and Na, $2.1m$ in K, and $2.3m$ in Rb. Using a phonon-broadened momentum distribution the data would yield for sodium $m^*/m \sim 1.4$–1.6, in fair agreement with calculations giving 1.2.

The positron thermalization was found to be complete at temperatures above about 100 °K in Li, 80 °K in Na, 50 °K in K, and 30 °K in Rb. Below these temperatures positrons seem to annihilate with certain minimum effective temperatures. Further measurements and calculations are needed for complete understanding of positron behavior at low temperatures.

ACKNOWLEDGMENTS

We wish to acknowledge J. B. Shand, J. J. Donaghy, and J. H. Kusmiss for the construction of the angular-correlation apparatus and J. P. Carbotte, B. Bergersen, and M. J. Scott for valuable discussions.

---

*Present address: Atomic Energy of Canada Ltd., Chalk River, Ontario, Canada.

†Present address: Department of Physics, Queen's University, Kingston, Ontario, Canada.

[1] *Positron Annihilation*, edited by A. T. Stewart and L. O. Roellig (Academic, New York, 1967).

[2] R. N. West, Adv. Phys. 22, 263 (1973).

[3] A. T. Stewart, J. B. Shand, J. J. Donaghy, and J. H. Kusmiss, Phys. Rev. 128, 118 (1962); J. B. Shand, Phys. Lett. A 30, 478 (1969).

[4] S. Berko, Phys. Rev. 128, 2166 (1962).

[5] J. J. Donaghy and A. T. Stewart, Phys. Rev. 164, 391 (1967).

[6] J. Melngailis and S. DeBenedetti, Phys. Rev. 145, 400 (1966).

[7] K. Fujiwara and O. Sueoka, J. Phys. Soc. Jpn. 21, 1949 (1966).

[8] S. Berko, S. Cushner, and J. C. Erskine, Phys. Lett. A 27, 668 (1968).

[9] J. C. Erskine and J. D. McGervey, Phys. Rev. 151, 615 (1966).

[10] D. Stroud and H. Ehrenreich, Phys. Rev. 171, 399 (1968).

[11] R. W. Williams and A. R. Mackintosh, Phys. Rev. 168, 679 (1968).

[12] R. P. Gupta and T. L. Loucks, Phys. Rev. 176, 848 (1968).

[13] S. M. Kim and W. J. L. Buyers, Can. J. Phys. 50, 1777 (1972).

[14] P. E. Mijnarends, Physica 63, 248 (1973).

[15] I. K. MacKenzie, T. L. Khoo, A. B. McDonald, and B. T. A. McKee, Phys. Rev. Lett. 19, 946 (1967).

[16] K. Fujiwara, O. Sueoka, and T. Imura, J. Phys. Soc. Jpn. 24, 467 (1968).

[17] B. W. Murray and J. D. McGervey, Phys. Rev. Lett. 24, 9 (1970).

[18] W. Trifthäuser and A. T. Stewart, J. Phys. Chem. Solids 32, 2717 (1971).

[19] A. Thompson, B. W. Murray, and S. Berko, Phys. Lett. A 37, 461 (1971).

[20] S. Berko and M. Weger, Phys. Rev. Lett. 24, 55 (1970).

[21] D. Schoenberg, in *The Physics of Metals*, edited by J. M. Ziman (Cambridge U. P., London, 1969), Vol. 1, p. 62.

[22] B. T. A. McKee, W. Trifthäuser, and A. T. Stewart, Phys. Rev. Lett. 28, 358 (1972).

[23] S. M. Kim, W. J. L. Buyers, P. Martel, and G. M. Hood, J. Phys. F 4, 343 (1974).

[24] A. Seeger, J. Phys. F 3, 248 (1973).

[25] I. K. MacKenzie, R. R. Gingerich, and S. M. Kim, in *Proceedings of the Second Conference on Positron Annihilation, Kingston, Ontario*, 1971, p. 459 (unpublished).

[26] C. L. Snead, Jr., T. M. Hall, and A. N. Goland, Phys. Rev. Lett. 29, 62 (1972).

[27] C. L. Snead, A. N. Goland, J. H. Kusmiss, H. C. Huang, and R. Meade, Phys. Rev. B 3, 275 (1971).

[28] R. M. J. Cotterill, I. K. MacKenzie, L. Smedskjer, G. Trumpy, and J. H. O. Träff, Nature 239, 99 (1972).

[29] R. M. J. Cotterill, K. Petersen, G. Trumpy, and J. Träff, J. Phys. F 2, 459 (1972).

[30] A. T. Stewart, Can. J. Phys. 35, 168 (1957).

[31]L. Hedin and S. Lundquist, in *Solid State Physics*, edited by H. Ehrenreich, F. Seitz, and D. Turnbull (Academic, New York, 1969), Vol. 23, p. 162.
[32]R. A. Ferrell, Rev. Mod. Phys. 28, 308 (1956).
[33]S. Kahana, Phys. Rev. 129, 1622 (1963).
[34]J. P. Carbotte and S. Kahana, Phys. Rev. 139, A213 (1965).
[35]J. P. Carbotte, Phys. Rev. 155, 197 (1967).
[36]J. Arponen and P. Jauho, Phys. Rev. 167, 239 (1968).
[37]B. Bhattacharyya and K. S. Singwi, Phys. Rev. Lett. 29, 22 (1972).
[38]D. R. Hamann, Phys. Rev. 146, 277 (1966).
[39]B. Bergersen and E. Pajanne, Phys. Rev. 186, 375 (1969).
[40]B. Bergersen and E. Pajanne, Phys. Rev. B 3, 1588 (1971).
[41]G. E. Lee-Whiting, Phys. Rev. 97, 1557 (1955).
[42]J. P. Carbotte and H. J. Arora, Can. J. Phys. 45, 387 (1967).
[43]E. J. Woll and J. P. Carbotte, Phys. Rev. 164, 985 (1967).
[44]R. E. Bell and M. H. Jorgensen, Can. J. Phys. 38, 652 (1960).
[45]J. J. Donaghy and A. T. Stewart, Phys. Rev. 164, 396 (1967).
[46]A. T. Stewart and J. B. Shand, Phys. Rev. Lett. 16, 261 (1966).
[47]A. T. Stewart, J. B. Shand, and S. M. Kim, Proc. Phys. Soc. Lond. 88, 1001 (1966).
[48]C. K. Majumdar, Phys. Rev. 149, 406 (1966).
[49]H. J. Mikeska, Z. Phys. 232, 159 (1970).
[50]A. Perkins and J. P. Carbotte, Phys. Rev. B 1, 101 (1970).
[51]P. R. Wallace, in *Solid State Physics*, edited by F. Seitz and D. Turnbull (Academic, New York, 1960), Vol. 10, p. 1.
[52]S. M. Kim, A. T. Stewart, and J. P. Carbotte, Phys. Rev. Lett. 18, 385 (1967).
[53]S. M. Kim, Ph.D. thesis (University of North Carolina, 1967) (unpublished).
[54]G. Knop and W. Paul, in *Alpha-, Beta-, and Gamma-Ray Spectroscopy*, edited by K. Siegbahn (North-Holland, Amsterdam, 1965), Vol. 1, p. 23.
[55]W. B. Pearson, *Handbook of Lattice Spacings and Structure of Metals and Alloys* (Pergamon, New York, 1958).
[56]C. K. Majumdar, Phys. Rev. 140, A227 (1965).
[57]W. Brandt and H. F. Waung, Phys. Lett. A 27, 700 (1968).
[58]C. H. Hodges, Phys. Rev. Lett. 25, 284 (1970).
[59]I. K. MacKenzie, T. W. Craig, and B. T. A. McKee, Phys. Lett. A 36, 227 (1971).
[60]B. B. J. Hede and J. P. Carbotte, Can. J. Phys. 48, 2661 (1970).
[61]C. S. Barrett, *Structure of Metals* (McGraw-Hill, New York, 1952).